Nonreciprocal coherent coupling of nanomagnets by exchange spin waves

Wang, Hanchen; Chen, Jilei; Yu, Tao; Liu, Chuanpu; Guo, Chenyang; Liu, Song; Shen, Ka; Jia, Hao; Bauer, Gerrit E.W.

DOI
10.1007/s12274-020-3251-5

Publication date
2020

Document Version
Accepted author manuscript

Published in
Nano Research

Nonreciprocal coherent coupling of nanomagnets by exchange spin waves

Hanchen Wang, Jilei Chen, Tao Yu, Chuanpu Liu, Chenyang Guo, Song Liu, Ka Shen, Hao Jia, Tao Liu, Jianyu Zhang, Marco A. Cabero Z, Qiuming Song, Sa Tu, Mingzhong Wu, Xiufeng Han, Ke Xia, Dapeng Yu, Gerrit E. W. Bauer, and Haiming Yu*

Beihang University, China

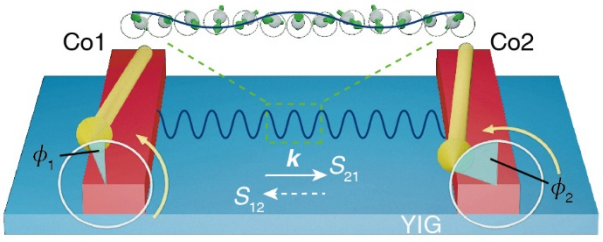

Two distant nanomagnets are unidirectionally phase-locked by propagating spin waves with sub-50 nm wavelengths.

Haiming Yu,
http://shi.buaa.edu.cn/hyu

Mingzhong Wu,
https://www.physics.colostate.edu/about/people/mingzhong-wu/

Xiufeng Han,
http://maglab.iphy.ac.cn/M02_Webpage/ch/people/XFHan-Chinese.htm

Ke Xia
https://www.sustech.edu.cn/zh/xiake.html

Dapeng Yu,
https://www.sustech.edu.cn/zh/yudapeng.html

Gerrit E.W. Bauer,
https://www.tudelft.nl/en/faculty-of-applied-sciences/about-faculty/departments/quantum-nanoscience/prof-dr-gerrit-bauer/

Nano Research

ISSN 1998-0124 CN 11-5974/O4
https://doi.org/(automatically inserted by the publisher)

Research Article

Nonreciprocal coherent coupling of nanomagnets by exchange spin waves

Hanchen Wang[1,§], Jilei Chen[1,§], Tao Yu[2,§], Chuanpu Liu[1,§], Chenyang Guo[3,§], Song Liu[4,§], Ka Shen[5,§], Hao Jia[4,§], Tao Liu[6], Jianyu Zhang[1], Marco A. Cabero Z[4,1], Qiuming Song[4], Sa Tu[1], Mingzhong Wu[6], Xiufeng Han[3], Ke Xia[4], Dapeng Yu[4], Gerrit E. W. Bauer[7,8,9], and Haiming Yu[1] (✉)

[1]*Fert Beijing Institute, School of Microelectronics, Beijing Advanced Innovation Center for Big Data and Brain Computing, Beihang University, Beijing 100191, China*
[2]*Max Planck Institute for the Structure and Dynamics of Matter, 22761 Hamburg, Germany*
[3]*Beijing National Laboratory for Condensed Matter Physics, Institute of Physics, University of Chinese Academy of Sciences, Chinese Academy of Sciences, Beijing 100190, China*
[4]*Shenzhen Institute for Quantum Science and Engineering (SIQSE), and Department of Physics, Southern University of Science and Technology (SUSTech), Shenzhen 518055, China*
[5]*Department of Physics, Beijing Normal University, Beijing 100875, China*
[6]*Department of Physics, Colorado State University, Fort Collins, Colorado 80523, USA*
[7]*Kavli Institute of Nanoscience, Delft University of Technology, 2628 CJ Delft, The Netherlands*
[8]*Institute for Materials Research, WPI-AIMR and CSNR, Tohoku University, Sendai 980-8577, Japan*
[9]*Zernike Institute for Advanced Materials, University of Groningen, Groningen, Nijenborgh 4, 9747 AG Groningen, The Netherlands*
[§]*Hanchen Wang, Jilei Chen, Tao Yu, Chuanpu Liu, Chenyang Guo, Song Liu, Ka Shen and Hao Jia contributed equally to this work*

ABSTRACT

Nanomagnets are widely used to store information in non-volatile spintronic devices. Spin waves can transfer information with low-power consumption as their propagation are independent of charge transport. However, to dynamically couple two distant nanomagnets via spin waves remains a major challenge for magnonics. Here we experimentally demonstrate coherent coupling of two distant Co nanowires by fast propagating spin waves in an yttrium iron garnet thin film with sub-50 nm wavelengths. Magnons in two nanomagnets are unidirectionally phase-locked with phase shifts controlled by magnon spin torque and spin-wave propagation. The coupled system is finally formulated by an analytical theory in terms of an effective non-Hermitian Hamiltonian. Our results are attractive for analog neuromorphic computing that requires unidirectional information transmission.

KEYWORDS

spintronics, nanomagnets, spin waves, coherent coupling, nonreciprocity

1 Introduction

Coupled nanomagnets offer a variety of functionalities towards non-volatile memories and logic gates and form essential building blocks for spintronic devices [1-4]. The interlayer exchange coupling between magnetic layers leads to the discovery of the giant magnetoresistance [5-7] and stimulates the broad applications of magnetic tunnel junctions [8-10]. Very recently, the nanomagnets are laterally coupled via the Dzyaloshinskii-Moriya interaction, where two static magnetic domains are connected through a chiral domain wall [11]. In addition to static magnetic coupling, GHz magnetization dynamics of nanomagnets can be coupled via e.g. dynamic exchange coupling [13] and dynamic dipolar coupling [14, 15]. However, these magnetic couplings are quickly weakened when the nanomagnets are separated apart. The dynamics of distant nanomagnets can be synchronized using an electrical current due to the spin-transfer torque effect [16, 17], which has important technological implications *e.g.* microwave generators [18-21]. Yet, a high current density is required to activate the synchronization, which would inevitably produce significant energy dissipation due to the Joule heating. Spin waves or its quanta, the magnons [22-31], are collective excitations of the magnetic order and can convey information free of charge transport. Therefore, spin waves are regarded as a promising candidate for the next-generation information carriers with low-power consumption. Magnons and photons are both bosons [32, 33], but have different dispersion relations: at the same frequencies magnons have much shorter wavelengths than photons, which offers spin waves an innate advantage for integrated nanodevices [34-38]. Incoherent-magnon-mediated coupling between magnets are found in the magnon valves with both vertical [39, 40] and lateral [41] structures. However, the long-distance coherent coupling between two nanomagnets via propagating spin waves has not been achieved yet.

Here, we experimentally demonstrate a nonreciprocal coupling of two distant ultra-thin film Co nanowires (>50 nm wide) that is mediated by fast exchange spin waves in 20 nm-thin yttrium

Address correspondence to Haiming Yu, haiming.yu@buaa.edu.cn.

iron garnet (YIG) films. Nonreciprocal spin waves are of great interest in magnonic applications due to the controllable wave flow for the transfer of information and logic functions [47-50]. The excitation and detection of coherent exchange spin waves is non-trivial by itself [46-49]. In this work, coherent exchange spin waves are excited with wavelengths down to $\lambda = 48$ nm, which are fastest reported so far [50-52] (see Electronic Supplementary Material (ESM)). More importantly, the Co wires are coherently and unidirectionally coupled by propagating spin waves with a phase shift $\Delta\phi$ that is freely tunable from 0 to 2π by propagation-induced phase delay. The coupling of spin waves in Co and YIG can be interpreted as a dynamic interlayer magnon spin torque [53-56] and the strong nonreciprocity is caused by the chiral spin pumping [57, 58], and not the intrinsic nonreciprocity of magnetostatic surface waves in thick magnetic slabs [59-61]. Theoretically, the coupled system of two Co wires and magnetic substrate can be formulated in terms of an effective non-Hermitian Hamiltonian [62-64]. The coupling strongly enhances the spin-wave mediated transmission signal [65], quite different from the level attraction of magnon and photon levels reported in a microwave cavity [66, 67].

2 Nanomagnonic device information

Figure 1(a) illustrates two identical Co nanowires in direct contact with a 20 nm-thin YIG film. The Co wires are 30 nm thin, 100 nm wide and separated by 1.5 μm. A scanning electron microscope (SEM) image is shown in Fig. 1(c). Magnons in two Co wires are coupled through spin waves in the YIG film with low magnetic damping [68, 69]. On each Co wires, gold nano-stripline (NSL) antennas (200 nm wide) [70] are integrated to coherently excite and detect spin waves (Fig. 1(b)). The microwave reflection spectrum S_{11} (Fig. 2(a)) is sensitive to the ferromagnetic resonance (FMR) of the material close to NSL1. The Co wire Kittel mode is observed at frequencies (14.5~19.5 GHz) much higher than that of the YIG film (0.5~3.5 GHz) due to the large form anisotropy of Co nanowires [71, 72]. An in-plane magnetic field H is applied parallel to Co wires. By sweeping H from negative to positive values, the magnetic configuration of Co/YIG device switches from parallel (P) to antiparallel (AP) because of the high coercivity of Co nanowires [71, 72] compared to the YIG film, returning to a parallel configuration only at $H > 50$ mT.

Microwaves are transmitted from Co1 to Co2 via propagating spin waves [25, 28, 69, 73] as measured by the transmission spectra S_{21} (its imaginary part is shown in Fig. 2(b)). We observe remarkable interference fringes (ripples) around the Co resonance in the AP state. The features in S_{21} (Fig. 2(b)) vanish in the reverse transmission spectra S_{12} (Fig. 1(f)), revealing a nearly perfect chiral excitation of exchange spin waves by the magnetodipolar fields from the Co nanowires [15, 57, 58]. This can be understood by the stray fields generated by the right (left) moving spin waves that vanish below (above) the film and precess in the opposite direction of the magnetization. Figure 2(d) is a cross section from S_{21} extracted at a field of 30 mT. The Co FMR related signal near 15 GHz is more than 10 times stronger than the signal at lower frequencies assigned to dipolar magnons close the FMR of YIG [74, 75]. Therefore, the short-wavelength, exchange-dominated magnons with high group velocities [47-52] transmit signals between two Co wires at high frequencies (14~17 GHz) and in one direction only.

3 Results and discussion

The mechanism of nonreciprocal coupling is conceptually sketched in Fig. 3(a). Due to the chiral spin pumping [58], the FMR of Co wire 1 can only couple to spin waves in YIG with wavevector k in one direction. After propagating over a finite distance d, the spin waves in YIG then drive the magnetization in Co wire 2 to precess. We find a fixed phase relation $\Delta\phi = \phi_2 - \phi_1$ between the spin precessions of two Co wires that is caused by: (1) Twice a shift of ϕ_i by the dynamical coupling [53-55] between the Co wires and YIG film, i.e. from Co1 to YIG and from YIG to Co2, which depends on the frequency. At resonance this process is purely dissipative, *i.e.* $\phi_i = \pi/2$; (2) the phase delay ϕ_k by the propagation of exchange spin waves with a finite wavenumber k over a distance d. The total phase-difference between the Kittel modes of Co2 and Co1, thus reads (see ESM)

$$\begin{aligned} \langle \hat{m}_2 \rangle &= \frac{2|\sigma_k|}{\frac{\kappa_{Co}}{2} + |\sigma_k|} e^{i\Delta\phi} \langle \hat{m}_1 \rangle, \\ \Delta\phi &= 2\phi_i + \phi_k, \\ \phi_i &= \frac{\pi}{2}, \\ \phi_k &= kd, \end{aligned} \tag{1}$$

in which $\langle \hat{m}_2 \rangle$ ($\langle \hat{m}_1 \rangle$) are coherent amplitudes of the Kittel magnons in Co2 (Co1), σ_k additional damping induced by the interface Zeeman coupling (see ESM), $\kappa_{Co} = 2\omega\alpha_G$ the reciprocal lifetime proportional to the Gilbert damping parameter α_G of the Co wires. The blue dashed line in Fig. 3(b) traces a mode of exchange spin waves with short wavelengths propagating in YIG [50]. When the propagating spin-wave mode crosses the Co resonance (red dashed line in Fig. 3(b)), the phase shifts by π and the transmission amplitude changes sign (yellow area of Fig. 3(c)). The non-locally excited Co2 can again pump spin waves (to the right) with a phase $\Delta\phi = 3\phi_i + \phi_k$ that destructively interferes with the waves coming from Co1 that have not been absorbed by Co2. Figure 3(d) shows a spectrum extracted along the Co FMR (red dashed line in Fig. 3(b)) with $2\phi_i = \pi$. The periodicity of the oscillations is caused by the propagation phase delay $\phi_k = kd$. Between two neighboring peaks (marked by red and blue arrows) $\Delta\phi = 2\pi$. Since the propagation distance d is fixed, the phase change is governed by the wavenumber variation $\Delta k = k_2 - k_1$ for the peak frequencies f_1 and f_2 [73]. The dispersion relation of dipole-exchange spin waves [76] in the Damon-Eshbach configuration for a 20 nm-thick YIG film [68, 69] is plotted in Fig. 3(e). Here, the value of the exchange constant $A = 3 \times 10^{-12}$ cm^2 is taken for ultrathin films [77]. From the dispersions, $k_1 =$ 89.9 rad μm^{-1}, $k_2 =$ 93.9 rad μm^{-1} and $\Delta k =$4.0 rad μm^{-1}, or $\phi_k = \Delta k \cdot d = 6.0$, which is reasonably close to 2π considering the uncertainty in d introduced by the finite width $w \approx 100$ nm of the wires. Micromagnetic simulations provide further support for coherent phase transfer between Co magnetizations (see ESM). Figures 3(f) and 3(g) show the dynamics of the y component of the wire

magnetization as indicated in the insets, which precesses either in phase $\Delta\phi = 0$ (Fig. 3(f)) or with $\Delta\phi = \pi/2$ (Fig. 3(g)), as a function of H and f.

S_{21} depends on the propagation distance d via the spin-wave propagation phase delay $\phi_k = k \cdot d$ as illustrated in Figs. 4(a-c) for a wire width $w =$ 60 nm (see ESM). The spin-wave group velocity $v_g = \frac{d\omega}{dk} = \frac{2\pi f}{k} = \frac{2\pi}{\Delta\phi_k}\Delta f \cdot d$, where Δf is the peak-to-peak frequency difference as shown *e.g.* in the inset of Fig. 4(d) (a cut of Fig. 4(a) at zero field) that corresponds to $\Delta\phi_k = d\Delta k = 2\pi$ and $v_g = \Delta f \cdot d$ or $\Delta f = v_g(1/d)$. Figure. 4(d) shows the observed Δf as a function of $1/d$ derived from Fig. 3(a)-3(c). Using the group velocity for dipole-exchange magnons [74] leads to a linear relationship between Δf and $1/d$ (blue dotted line in Fig. 4(d)) that deviates significantly from the experimental data. However, taking $\phi_i = \pi/2$ into account, $\phi_k = \Delta\phi - 2\phi_i$ and $\Delta f = \frac{1}{2}v_g(1/d)$. This leads to the red solid line in Fig. 4(d) that agrees nicely with experimental data.

S_{21} for $w =$ 60 nm shows a clear beating pattern for all d that leads to a vanishing oscillation around 19 GHz (white arrow in Fig. 4(b)) that do not show up for w =100 nm sample (Fig. 3(b)). Indeed, we argue that the interlayer coupling strength g_k should depend on the wire width (see ESM). The Hamiltonian for a single wire close to the film can be written as

$$\frac{\hat{\mathcal{H}}_{\mathrm{Co|YIG}}}{\hbar} = \omega^{\mathrm{Co}}\hat{m}^{\dagger}\hat{m} + \sum\nolimits_k \omega_k^{\mathrm{YIG}}\hat{p}_k^{\dagger}\hat{p}_k + \sum\nolimits_k \left(g_k\hat{m}\hat{p}_k^{\dagger} + g_k^{*}\hat{m}^{\dagger}\hat{p}_k\right), \tag{2}$$

where $\hat{m}$ and $\hat{p}_k$ are bosonic operators associated, respectively, with the Kittel mode in Co and spin waves in YIG with wavenumber k. ω^{Co} is the Co FMR frequency, ω_k^{YIG} the YIG spin-wave frequency dispersion [74] (see ESM). The interlayer coupling matrix elements g_k can be caused by the interface exchange or magnetodipolar interaction. The indirect Co-Co coupling strength as sketched in Fig. 2(a) scales with $|g_k|^2 \propto \left|\int_0^w e^{iky}\,dy\right|^2 = \left|\frac{\sin(kw/2)}{k/2}\right|^2$, which is plotted as a function of wavelength $\lambda = 2\pi/k$ in Fig. 3(f) (see ESM). The blue shaded interval $\lambda =$ 54.0~66.8 nm corresponds to the spectrum plotted in Fig. 3(e) (see ESM). In this range, the relative coupling strength shows a minimum around 60 nm (Fig. 4(e)), which explains the suppressed amplitude around 19 GHz (Figs. 4(a-c)). In the w =100 nm sample (Fig. 3(d)), we also observe some amplitude modulation (see ESM). The experimental results shown in Fig. 4(b) may be directly compared with the calculated transmission based on the theoretical analysis [12, 78-80] (see ESM).

The coherent excitation of Co2 from Co1 is driven by a magnon spin torque [53-56] mediated by exchange spin waves in the YIG film. The torque transferred at Co1|YIG and YIG|Co2 may be induced by either interfacial exchange or magnetodipolar coupling. In view of an interfacial exchange coupling strength measured to be 0.2 GHz in planar Co|YIG films [53], the exchange coupling strength at the interface between a single Co nanowire and the YIG film is merely 20 kHz, which is negligible in comparison with the magnetodipolar coupling calculated and shown in Fig. 4(f). It has been theoretically studied that the interlayer exchange (magnetodipolar) coupling is larger at the parallel (antiparallel) configuration [58]. The experimental observation that strong transmission between Co1 and Co2 occurs at the antiparallel configuration (Fig. 2(b)) indicates that the magnetodipolar interaction is responsible for the coupling at Co1|YIG and YIG|Co2. The dominance of magnetodipolar coupling and the absence of interlayer exchange give rise to the spin-wave chirality and eventually lead to the nonreciprocal coupling of two Co wires. A chiral spin pumping can also be achieved by microwaves emitted by normal metal antennas that can couple to the dipolar spin waves in thick films [81]. However, this process is very inefficient in ultrathin films, while the exchange spin waves as excited by magnetic nanowires here cannot be accessed at all. Theoretically, the coupling between two Co wires can be described by an effective Hamiltonian as

$$\begin{aligned}
\frac{\hat{\mathcal{H}}_{\mathrm{Co|Co}}}{\hbar} &= \sum_{i=1}^{2}(\omega_l^{\mathrm{Co}} - i\Gamma_l)\hat{m}_l^{\dagger}\hat{m}_l - i\Gamma_{12}(\omega)\hat{m}_1^{\dagger}\hat{m}_2 - i\Gamma_{21}(\omega)\hat{m}_2^{\dagger}\hat{m}_1, \\
\Gamma_{l=1,2}(\omega) &\equiv -\int\frac{dk}{2\pi}\frac{|g_{k,l}|^2}{i(\omega-\omega_k)-\frac{\kappa_{\mathrm{YIG}}}{2}}, \\
\Gamma_{12}(\omega) &\equiv -\int\frac{dk}{2\pi}\frac{g_{+k,1}g_{+k,2}^{*}}{i(\omega-\omega_k)-\frac{\kappa_{\mathrm{YIG}}}{2}}, \\
\Gamma_{21}(\omega) &\equiv -\int\frac{dk}{2\pi}\frac{g_{-k,1}^{*}g_{-k,2}}{i(\omega-\omega_k)-\frac{\kappa_{\mathrm{YIG}}}{2}}.
\end{aligned} \tag{3}$$

where Γ_{12} (Γ_{21}) is the coupling from Co1 (2) to Co2 (1), κ_{YIG} stands for the FMR linewidth of the YIG film, $g_{+k,1}$ ($g_{+k,2}$) the coupling between Co1 (2) and propagating spin waves in YIG with positive wavenumber $+k$, $g_{-k,1}$ ($g_{-k,2}$) the coupling strength between Co1 (2) and spin waves with $-k$. Here the spin-wave coupling is chiral, $g_{-k,1} = 0$ and $g_{-k,2} = 0$, as illustrated in Fig. 3(a) [57, 58] and $\Gamma_{12} \approx 0$ and hence Eq. 3 is non-Hermitian.

4 Conclusions

In summary, we have demonstrated on-chip nonreciprocal coupling of two distant nanomagnets at room temperature. The two Co wires are found to be phase-related by propagating exchange spin waves in the YIG film. Any desired phase shift $\Delta\phi$ from 0 to 2π can be realized by tuning frequencies and applied magnetic fields in the vicinity of the Co FMR. The magnon transmission varies sensitively with propagation distance and the nanowire width, providing additional evidence for the phase-coherent coupling. We theoretically describe the coupling between two Co wires in terms of a Hamiltonian that includes the chiral spin pumping and therefore becomes non-Hermitian [58]. This formulation helps to predict new phenomena, such as the magnon trap [82] and chiral magnetic noise [83]. The chiral coupling of nanomagnets demonstrated in this work is attractive for neuromorphic computing [84, 85], since it mimics the innately unidirectional information transmission between neurons via synapses [86].

Acknowledgements

The authors thank L. Flacke, M. Althammer, M. Weiler, K. Schultheiss, H. Schultheiss, M. Madami, G. Gubbiotti and C.M. Hu for their helpful discussions. Funding: We wish to acknowledge the support by NSF China under Grants No. 11674020, No. 12074026 and No. U1801661, the 111 talent program B16001,

the National Key Research and Development Program of China Grants No. 2016YFA0300802 and No. 2017YFA0206200. G.B. was supported by the Netherlands Organization for Scientific Research (NWO) and Japan Society for the Promotion of Science Kakenhi Grants-in-Aid for Scientific Research (Grant No. 19H006450). T. Y. was funded through the Emmy Noether Program of Deutsche Forschungsgemeinschaft (SE 2558/2-1). K.X. thanks the National Key Research and Development Program of China (Grants No. 2017YFA0303304 and No. 2018YFB0407601) and the National Natural Science Foundation of China (Grants No. 61774017 and No. 11734004). K.S. was supported by the Fundamental Research Funds for the Central Universities (Grant No. 2018EYT02). C.L. and M.Z.W. were supported by the US National Science Foundation (Grant No. EFMA-1641989).

Electronic Supplementary Material: Supplementary material (material characterization, device fabrication, measurement techniques, spin-wave dispersion at different fields, SEM images of the nanowires with different widths, coupling strength with different nanowire widths and wavenumbers, details of mircomagnetic simulations of chiral spin-wave emission, theory of spin-wave chiral dynamics including stripline magnetic field, magnon coupling by dipolar interaction, magnon damping by chiral spin pumping, phase relation between nanowires and non-Hermitian coupling and the shortest wavelength observed in the transmission spectra) is available in the online version of this article at http://dx.doi.org/10.1007/s12274-***-****-* (automatically inserted by the publisher).

References

[1]. Wolf, S. A.; Awschalom, D. D.; Buhrman, R. A.; Daughton, J. M.; von Molnár, S.; Roukes, M. L.; Chtchelkanova, A. Y.; Treger, D. M. Spintronics: A spin-based electronics vision for the future. *Science* **2001**, *294*, 1488-1495.

[2]. Imre, A.; Csaba, G.; Ji, L.; Orlov, A.; Bernstein, G. H.; Porod, W. Majority logic gate for magnetic quantum-dot cellular automata. *Science* **2006**, *311*, 205-208.

[3]. Fert, A. Nobel lecture: Origin, development, and future of spintronics. *Rev. Mod. Phys.* **2008**, *80*, 1517-1530.

[4]. Cui, J.; Huang, T. Y.; Luo, Z.; Testa, P.; Gu, H.; Chen, X.; Nelson, B. J.; Heyderman, L. J. Nanomagnetic encoding of shape-morphing micromachines. *Nature* **2020**, *578*, 164-168.

[5]. Baibich, M. N.; Broto, J. M.; Fert, A.; Nguyen Van Dau, F.; Petroff, F.; Etienne, P.; Creuzet, G.; Friederich, A.; Chazelas J. Giant Magnetoresistance of (001)Fe/(001)Cr Magnetic Superlattices. *Phys. Rev. Lett.* **1988**, *61*, 2472-2475.

[6]. Binasch, G.; Grünberg, P.; Saurenbach, F.; Zinn, W. Enhanced magnetoresistance in layered magnetic structures with antiferromagnetic interlayer exchange. *Phys. Rev. B* **1989**, *39*, 4828-4830.

[7]. Parkin, S. S. P.; More, N.; Roche, K. P. Oscillations in exchange coupling and magnetoresistance in metallic superlattice structures: Co/Ru, Co/Cr, and Fe/Cr. *Phys. Rev. Lett.* **1990**, 64, 2304-2307.

[8]. Moodera, J. S.; Kinder, L. R.; Wong, T. M.; Meservey, R. Large magnetoresistance at room temperature in ferromagnetic thin film tunnel junctions. *Phys. Rev. Lett.* **1995**, *74*, 3273-3276.

[9]. Wang, W.-G.; Li, M.; Hageman, S.; Chien, C. L. Electric-field-assisted switching in magnetic tunnel junctions. *Nat. Mater.* **2012**, *11*, 64-68.

[10]. Borders, W. A.; Pervaiz, A. Z.; Fukami, S.; Camsari, K. Y.; Ohno, H.; Datta, S. Integer factorization using stochastic magnetic tunnel junctions. *Nature*, **2020**, *573*, 390-393.

[11]. Luo, Z.; Dao, T.P.; Hrabec, A.; Vijayakumar, J.; Kleibert, A.; Baumgartner, M.; Kirk, E.; Cui, J.; Savchenko, T.; Krishnaswamy, G. et al. Chirally coupled nanomagnets. *Science* **2019**, *363*, 1435-1439.

[12]. Tserkovnyak, Y.; Brataas, A.; Bauer, G. E. W.; Halperin, B. I. Nonlocal magnetization dynamics in ferromagnetic heterostructures. *Rev. Mod. Phys.* **2005**, *77*, 1375-1421.

[13]. Heinrich, B.; Tserkovnyak, Y.; Woltersdorf, G.; Zhang, P.; Brataas A.; Urban, R.; Bauer G. E. W. Dynamic exchange coupling in magnetic bilayers. *Phys. Rev. Lett.* **2003**, *90*, 187601.

[14]. Pigeau, B.; Hahn, C.; De Loubens, G.; Naletov, V. V.; Klein, O.; Mitsuzuka, K.; Lacour, D.; Hehn, M.; Andrieu, S.; Montaigne, F. Measurement of the dynamical dipolar coupling in a pair of magnetic nanodisks using a ferromagnetic resonance force microscope. *Phys. Rev. Lett.* **2012**, *109*, 247602.

[15]. Yu, T.; Bauer, G. E. W. Chiral coupling to magnetodipolar radiation, arXiv: 2001.06821.

[16]. Slonczewski, J. Current-driven excitation of magnetic multilayers. *J. Magn. Magn. Mater.* **1996**, *159*, L1-L7.

[17]. Berger, L. Emission of spin waves by a magnetic multilayer traversed by a current. *Phys. Rev. B* **1996**, *54*, 9353.

[18]. Kaka, S.; Pufall, M. R.; Rippard, W. H.; Silva, T. J.; Russek, S. E.; Katine, J. A. Mutual phase-locking of microwave spin torque nano-oscillators. *Nature* **2005**, *437*, 389-392.

[19]. Madami, M.; Bonetti, S.; Consolo, G.; Tacchi, S.; Carlotti, G.; Gubbiotti, G.; Manco, F. B.; Yar, M. A.; Åkerman, J. Direct observation of a propagating spin wave induced by spin-transfer torque. *Nat. Nanotechnol.* **2011**, *6*, 635-638.

[20]. Demidov, V. E.; Urazhdin, S.; Ulrichs, H.; Tiberkevich, V.; Slavin, A.; Baither, D.; Schmitz, G.; Demokritov, S. O. Magnetic nano-oscillator driven by pure spin current. *Nat. Mater.* **2012**, *11*, 1028-1031.

[21]. Urazhdin, S.; Demidov, V. E.; Ulrichs, H.; Kendziorczyk, T.; Kuhn, T.; Leuthold, J.; Wilde, G.; Demokritov, S. O. Nanomagnonic devices based on the spin-transfer torque. *Nat. Nanotechnol.* **2014**, *9*, 509-513.

[22]. Kruglyak, V. V.; Demokritov, S. O.; Grundler, D. Magnonics. *J. Phys. D: Appl. Phys.* **2010**, *43*, 264001.

[23]. Lenk, B.; Ulrichs, H.; Garbs, F.; Münzenberg, M. The building blocks of magnonics. *Phys. Rep.* **2011**, *507*, 107-136.

[24]. Chumak, A. V.; Vasyuchka, V. I.; Serga, A. A.; Hillebrands, B. Magnon spintronics. *Nat. Phys.* **2015**, *11*, 453-461.

[25]. Vlaminck, V.; Bailleul, M. Current-induced spin wave Doppler shift. *Science* **2008**, *322*, 410-413.

[26]. Vogt, K.; Fradin, F. Y.; Pearson, J. E.; Sebastian, T.; Bader, S. D.; Hillebrands, B.; Hoffmann, A.; Schultheiss, H. Realization of a spin-wave multiplexer. *Nat. Commun.* **2014**, *5*, 3727.

[27]. Pal, S.; Saha, S.; Kamalakar, M. V.; Barman, A. Field-dependent spin waves in high-aspect-ratio single-crystal ferromagnetic nanowires. *Nano Res.* **2016**, *9*, 1426-1433.

[28]. Han, J. H.; Zhang, P. X.; Hou, J. T.; Siddiqui, S. A.; Liu, L. Q. Mutual control of coherent spin waves and magnetic domain walls in a magnonic device. *Science* **2019**, *366*, 1121-1125.

[29]. Wang, Y.; Zhu, D.; Yang, Y.; Lee, K.; Mishra, R.; Go, G.; Oh, S.-H.; Kim, D.-H.; Cai, K.; Liu, E. et al. Magnetization switching by magnon-mediated spin torque through an antiferromagnetic insulator. *Science* **2019**, *366*, 1121-1125.

[30]. Yu, W. C.; Lan, J.; Xiao, J. Magnetic logic gate based on polarized spin waves. *Phys. Rev. Appl.* **2020**, *13*, 024055.

[31]. Heinz, B.; Brächer, T.; Schneider, M.; Wang, Q.; Lägel, B.; Friedel, A. M.; Breitbach, D.; Steinert, S.; Meyer, T.; Kewenig, M. et al. Propagation of spin-wave packets in individual nanosized yttrium iron garnet magnonic conduits. *Nano Lett.* **2020**, *20*, 4220-4227.

[32]. Demokritov, S.; Demidov, V. E.; Dzyapko, O.; Melkov, G. A.; Serga, A. A.; Hillebrands, B.; Slavin, A. N. Bose-Einstein condensation of quasi-equilibrium magnons at room temperature under pumping. *Nature* **2006**, *443*, 430-433.

[33]. Schneider, M.; Brächer, T.; Breitbach, D.; Lauer, V.; Pirro, P.; Bozhko, D. A.; Musiienko-Shmarova, H. Y.; Heinz, B.; Wang, Q.; Meyer, T. et al. Bose Einstein condensation of quasiparticles by rapid cooling. *Nat. Nanotechnol.* **2020**, *15*, 457-461.

[34]. Khitun, A.; Bao, M.; Wang, K. L. Magnonic logic circuits. *J. Phys. D Appl. Phys.* **2010**, *43*, 264005.

[35]. Grundler, D. Spintronics: Nanomagnonics around the corner. *Nat. Nanotechnol.* **2016**, *11*, 407-408.

[36]. Wagner, K.; Kákay, A.; Schultheiss, K.; Henschke, A.; Sebastian, T.; Schultheiss, H. Magnetic domain walls as reconfigurable spin-wave nanochannels. *Nat. Nanotechnol.* **2016**, *11*, 432-436.

[37]. Halder, A.; Kumar, D.; Adeyeye, A. O. A recongurable waveguide for energy-ecient transmission and local manipulation of information in a

nanomagnetic device. *Nat. Nanotechnol.* **2016**, *11*, 437-443.
[38]. Csaba, G.; Porod, W. Coupled oscillators for computing: A review and perspective. *Appl. Phys. Rev.* **2020**, *7*, 011302.
[39]. Wu, H.; Huang, L.; Fang, C.; Yang, B. S.; Wan, C. H.; Yu, G. Q.; Feng, J. F.; Wei, H. X.; Han, X. F. Magnon valve effect between two magnetic insulators. *Phys. Rev. Lett.* **2018**, *120*, 097205.
[40]. Cramer, J.; Fuhrmann, F.; Ritzmann, U.; Gall, V.; Niizeki, T.; Ramos, R.; Qiu, Z.; Hou, D.; Kikkawa, T.; Sinova, J. et al. Magnon detection using a ferroic collinear multilayer spin valve. *Nat. Commun.* **2018**, *9*, 1089.
[41]. Cornelissen, L. J.; Liu, J.; Van Wees, B. J.; Duine, R. A. Spin-current-controlled modulation of the magnon spin conductance in a three-terminal magnon transistor. *Phys. Rev. Lett.* **2018**, *120*, 097702.
[42]. Khalili Amiri, P.; Rejaei, B.; Vroubel, M.; Zhuang, Y. Nonreciprocal spin wave spectroscopy of thin Ni-Fe stripes. *Appl. Phys. Lett.* **2007**, *91*, 062502.
[43]. Kwon, J. H.; Yoon, J.; Deorani, P.; Lee, J. M.; Sinha, J.; Lee, K.-J.; Hayashi, M.; Yang, H. Giant nonreciprocal emission of spin waves in Ta/Py bilayers. *Sci. Adv.* **2016**, *2*, e1501892.
[44]. Brächer, T.; Pirro, P.; Boulle, O.; Gaudin, G. Creation of unidirectional spin-wave emitters by utilizing interfacial Dzyaloshinskii-Moriya interaction. *Phys. Rev. B.* **2017**, *95*, 064429.
[45]. Henry, Y.; Stoeffle, D.; Kim, J.-V.; Bailleul, M. Unidirectional spin-wave channeling along magnetic domain walls of Bloch type. *Phys. Rev. B* **2019**, *100*, 024416.
[46]. Sandweg, C. W.; Kajiwara, Y.; Chumak, A. V.; Serga, A. A.; Vasyuchka, V. I.; Jungfleisch, M. B.; Saitoh, E.; Hillebrands, B. Spin pumping by parametrically excited exchange magnons. *Phys. Rev. Lett.* **2011**, *106*, 216601.
[47]. Wintz, S.; Erbe, A.; Tiberkevich, V.; Weigand, M.; Raabe, J.; Lindner, J.; Slavin, A.; Fassbender, J. Magnetic vortex cores as tunable spin-wave emitters. *Nat. Nanotechnol.* **2016**, *11*, 948-953.
[48]. Hämäläinen, S. J.; Brandl, F.; Franke, K. J. A.; Grundler, D.; van Dijken, S. Tunable short-wavelength spin-wave emission and confinement in anisotropy-modulated multiferroic heterostructures. *Phys. Rev. Applied* **2017**, *8*, 014020.
[49]. Brächer, T.; Fabre, M.; Meyer, T. ; Fischer, T. ; Auffret, S. ; Boulle, O. ; Ebels, U. ; Pirro, P. ; Gaudin, G. Detection of short-waved spin waves in individual microscopic spin-wave waveguides using the inverse spin Hall effect. *Nano Lett.* **2017**, *17*, 7234-7241.
[50]. Liu, C.; Chen, J.; Liu, T.; Heimbach, F.; Yu, H.; Xiao, Y.; Hu, J.; Liu, M.; Chang, H.; Stueckler, T. et al. Long-distance propagation of shortwavelength spin waves. *Nat. Commun.* **2018**, *9*, 738.
[51]. Dieterle, G.; Förster, J.; Stoll, H.; Semisalova, A. S.; Finizio, S.; Gangwar, A.; Weigand, M.; Noske, M.; Fähnle, M.; Bykova, I. et al. Coherent excitation of heterosymmetric spin waves with ultrashort wavelengths. *Phys. Rev. Lett.* **2019**, *122*, 117202.
[52]. Che, P.; Baumgaertl, K.; Kukolova, A.; Dubs, C.; Grundler, D. Efficient wavelength conversion of exchange magnons below 100 nm by magnetic coplanar waveguides. *Nat. Commun.* **2020**, *11*, 1445.
[53]. Klingler, S.; Amin, V.; Geprags, S.; Ganzhorn, K.; Maier-Flaig, H.; Althammer, M.; Huebl, H.; Gross, R.; McMichael, R. D.; Stiles, M. D. et al. Spin-torque excitation of perpendicular standing spin waves in coupled YIG/Co heterostructures. *Phys. Rev. Lett.* **2018**, *120*, 127201.
[54]. Chen, J.; Liu, C.; Liu, T.; Xiao, Y.; Xia, K.; Bauer, G. E. W.; Wu, M.; Yu, H. Strong interlayer magnon-magnon coupling in magnetic metal-insulator hybrid nanostructures. *Phys. Rev. Lett.* **2018**, *120*, 217202.
[55]. Qin, H.; Hämäläinen, S. J.; van Dijken, S. Exchange torque-induced excitation of perpendicular standing spin waves in nanometer-thick YIG films. *Sci. Rep.* **2018**, *8*, 5755.
[56]. Li, Y.; Cao, W.; Amin, V. P.; Zhang, Z.; Gibbons, J.; Sklenar, J.; Pearson, J.; Haney, P. M.; Stiles, M. D.; Bailey, W. E. et al. Coherent spin pumping in a strongly coupled magnon-magnon hybrid system. *Phys. Rev. Lett.* **2020**, *124*, 117202.
[57]. Chen, J.; Yu, T.; Liu, C.; Liu, T.; Madami, M.; Shen, K.; Zhang, J.; Tu, S.; Alam, M. S.; Xia, K. *et al.* Excitation of unidirectional exchange spin waves by a nanoscale magnetic grating. *Phys. Rev. B* **2019**, *100*, 104427.
[58]. Yu, T.; Blanter, Y. M.; Bauer, G. E. W. Chiral pumping of spin waves. *Phys. Rev. Lett.* **2019**, *123*, 247202.
[59]. Schneider, T.; Serga, A. A.; Neumann, T.; Hillebrands, B.; Kostylev, M. P. Phase reciprocity of spin-wave excitation by a microstrip antenna. *Phys. Rev. B* **2008**, *77*, 214411.
[60]. Demidov, V. E.; Kostylev, M. P.; Rott, K.; Krzysteczko, P.; Reiss, G.; Demokritov, S. O. Excitation of microwaveguide modes by a stripe antenna. *Appl. Phys. Lett.* **2009**, *95*, 112509.
[61]. Sekiguchi, K.; Yamada, K.; Seo, S. M.; Lee, K. J.; Chiba, D.; Kobayashi, K.; Ono, T. Nonreciprocal emission of spin-wave packet in FeNi film. *Appl. Phys. Lett.* **2010**, *97*, 022508.
[62]. El-Ganainy, R.; Makris, K. G.; Khajavikhan, M.; Musslimani, Z. H.; Rotter, S.; Christodoulides, D.N. Non-Hermitian physics and PT symmetry. *Nat. Phys.* **2018**, *14*, 11-19.
[63]. Miri, M.-A.; Alù, A. Exceptional points in optics and photonics. *Science* **2019**, *363*, eaar7709.
[64]. Carlström, J.; Stålhammar, M.; Budich, J. C.; Bergholtz, E. J. Knotted non-Hermitian metals. *Phys. Rev. B* **2019**, *99*, 161115(R).
[65]. Grigoryan, V. L.; Shen, K.; Xia, K. Synchronized spin photon coupling in a microwave cavity. *Phys. Rev. B* **2018**, *98*, 024406.
[66]. Harder, M.; Yang, Y.; Yao, B. M.; Yu, C. H.; Rao, J. W.; Gui, Y. S.; Stamps, R. L.; Hu, C.-M. Level attraction due to dissipative magnon-photon coupling. *Phys. Rev. Lett.* **2018**, *121*, 137203.
[67]. Yu, W. C.; Wang, J.; Yuan, H. Y.; Xiao, J. Prediction of attractive level crossing via a dissipative mode. *Phys. Rev. Lett.* **2019**, *113*, 227201.
[68]. Chang, H.; Li, P.; Zhang, W.; Liu, T.; Hoffmann, A.; Deng, L.; Wu. M. Nanometer-thick yttrium iron garnet films with extremely low damping. *IEEE Magn. Lett.* **2014**, *5*, 6700.
[69]. Yu, H.; d'Allivy Kelly, O.; Cros, V.; Bernard, R.; Bortolotti, P.; Anane, A.; Brandl, F.; Huber, R.; Stasinopoulos, I.; Grundler, D. Magnetic thin-film insulator with ultralow spin wave damping for coherent nanomagnonics. *Sci. Rep.* **2014**, *4*, 6848.
[70]. Ciubotaru, F.; Devolder, T.; Manfrini, M.; Adelmann, C.; Radu, I. P. All electrical propagating spin wave spectroscopy with broadband wavevector capability. *Appl. Phys. Lett.* **2016**, *109*, 012403.
[71]. Topp, J.; Heitmann, D.; Kostylev, M.P.; Grundler, D. Making a reconfigurable artificial crystal by ordering bistable magnetic nanowires. *Phys. Rev. Lett.* **2010**, *104*, 207205.
[72]. Ding, J.; Kostylev, M.; Adeyeye, A. O. Magnonic crystal as a medium with tunable disorder on a periodical lattice. *Phys. Rev. Lett.* **2011**, *107*, 047205.
[73]. Neusser, S.; Durr, G.; Bauer, H. G.; Tacchi, S.; Madami, M.; Woltersdorf, G.; Gubbiotti, G.; Back, C. H.; Grundler, D. Anisotropic propagation and damping of spin waves in a nanopatterned antidot lattice. *Phys. Rev. Lett.* **2010**, *105*, 067208.
[74]. Sun, Y. Y.; Song, Y. Y.; Chang, H.; Kabatek, M.; Jantz, M.; Schneider, W.; Gubbiotti, G.; Wu, M.; Schultheiss, H.; Hoffmann, A. Growth and ferromagnetic resonance properties of nanometer-thick yttrium iron garnet films. *Appl. Phys. Lett.* **2012**, *101*, 152405.
[75]. Serga, A. A.; Chumak, A. V.; Hillebrands, B. YIG magnonics. *J. Phys. D Appl. Phys.* **2010**, *43*, 264002.
[76]. Kalinikos, B. A.; Slavin, A. N. Theory of dipole exchange spin wave spectrum for ferromagnetic films with mixed exchange boundary conditions. *J. Phys. C Solid State Phys.* **1986**, *19*, 7013-7033.
[77]. Klingler, S.; Chumak, A. V.; Mewes, T.; Khodadadi, B.; Mewes, C.; Dubs, C.; Surzenko, O.; Hillebrands, B.; Conca, A. Measurements of the exchange stiffness of YIG films using broadband ferromagnetic resonance techniques. *J. Phys. D Appl. Phys.* **2015**, *48*, 015001.
[78]. Gardiner, C. W.; Collett, M. J. Input and output in damped quantum systems: Quantum stochastic differential equations and the master equation. *Phys. Rev. A* **1985**, *31*, 3761.
[79]. Clerk, A. A.; Devoret, M. H.; Girvin, S. M.; Marquardt, F.; Schoelkopf, R. J. Introduction to quantum noise, measurement, and amplification. *Rev. Mod. Phys.* **2010,** *82*, 1155.
[80]. Yu, T.; Bauer, G. E. W. Non-contact spin pumping by microwave evanescent fields. *Phys. Rev. Lett.* **2020**, *124*, 236801.
[81]. Wong, K. L.; Bi, L.; Bao, M.; Wen, Q.; Chatelon, J. P.; Lin, Y.-T.; Ross, C. A.; Zhang, H.; Wang, K. L. Unidirectional propagation of magnetostatic surface spin waves at a magnetic film surface. *Appl. Phys. Lett.* **2014**, *105*, 232403.
[82]. Yu, T.; Wang, H.; Sentef, M. A.; Yu, H.; Bauer, G. E. W. Magnon trap by chiral spin pumping. *Phys. Rev. B* **2020**, *102*, 054429.
[83]. Rustagi, A.; Bertelli, I.; van der Sar, T.; Upadhyaya, P. Sensing chiral magnetic noise via quantum impurity relaxometry. arXiv: 2009.05060v1.
[84]. Torrejon, J.; Riou, M.; Araujo, F. A.; Tsunegi, S.; Khalsa, G.; Querlioz, D.; Portolotti, P.; Cros, V.; Yakushiji, Y.; Fukushima A. et al. Neuromorphic computing with nanoscale spintronics oscillators. *Nature* **2017**, *547*, 428-431.
[85]. Zahedinejad, M.; Awad, A. A.; Muralidhar, S.; Khymyn, R.; Fulara, H.;

Mazraati, H.; Dvornik, M.; Åkerman, J. Two-dimensional mutually synchronized spin Hall nanooscillator arrays for neuromorphic computing. *Nat. Nanotechnol.* **2020**, *15*, 47-52.

[86]. Kandel, E. K.; Schwartz, J. H.; Jessel, T. M. *Principles of Neural Science;* McGraw-Hill/Appleton & Lange, 2000.

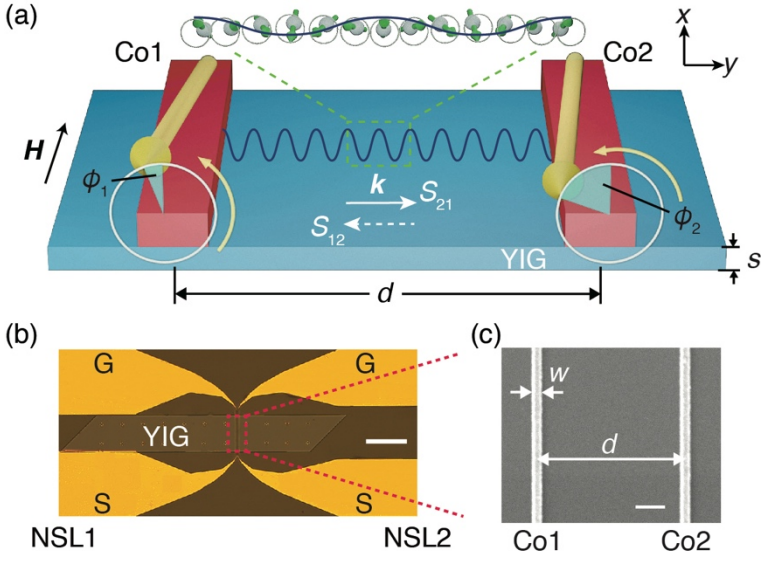

Figure 1 (a) A schematic diagram of two Co nanowires coupled by spin waves in the YIG film. Parameters are the film thickness s, the distance between the nanowires d, the spin-wave wavevector k and the in-plane applied field H. The coupling between Co1 (2) and Co2 (1) is evident in the microwave transmission spectra S_{21} (S_{12}) measured by nano-stripline antennas. The shift $\Delta\phi = \phi_2 - \phi_1$ of the precession phases of the Kittel modes in two wires can be controlled. (b) An optical microscope image of the device with two ground-signal antennas, NSL1 and NSL2. Scale bar, 100 μm. (c) An SEM image of two Co wires with width $w =$ 100 nm and center-to-center distance $d =$ 1.5 μm. Scale bar, 300 nm.

Figure 2 (a) Reflection spectra S_{11} measure the microwave absorption by NSL1. The ferromagnetic resonances of the Co wires and YIG film are indicated by white arrows. By sweeping the magnetic field H from negative to positive values, the magnetization of the Co/YIG bilayer switches from the parallel (P) to antiparallel (AP) magnetic configuration from 0 to 54 mT (white dashed lines). Transmission spectra S_{21} plotted in (b) exhibits strong spin-wave oscillations in the AP state close to the Co resonance. In the reversed transmission S_{12} (c) such oscillations are not detected. (d) is a line plot of the spectrum at 30 mT, tracing the yellow dashed line in (b), in which the blue and red areas represent the dipolar and exchange magnon regimes, respectively. The enhanced transmission signal indicated by the white arrow is caused by the coupling of the two Co wires through exchange magnons in YIG.

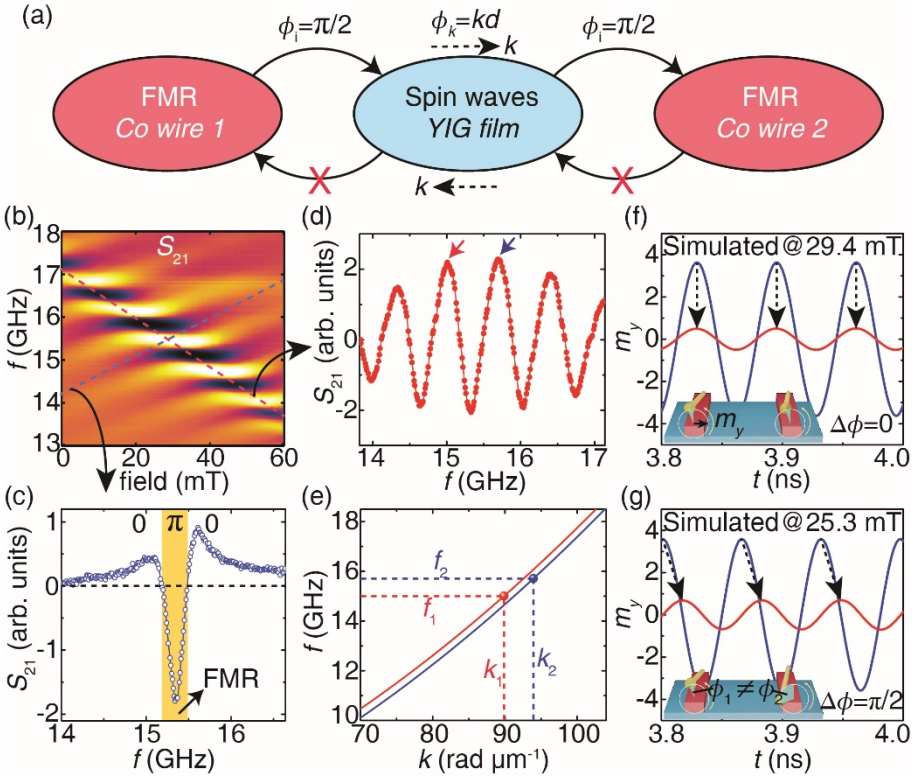

Figure 3 (a) A sketch of the phase-locking between two Co wires on top of a YIG film. A resonant Co wire imprints a dissipative phase shift $\phi_i = \pi/2$ on exciting spin waves below by the dipolar interaction. The phase delay due to the propagation of spin waves is given by $\phi_k = k \cdot d$. This coupling is unidirectional, which implies a non-Hermitian coupling. (b) Transmission spectra S_{21} measured at AP states of Co/YIG (close-up of Fig. 1e). (c) A single spectrum along the blue dashed line in (b) shows a phase change of π in the vicinity of the Co resonance (yellow region). (d) is S_{21} along the Co resonance, red-dashed line in (b). The frequencies of the transmission maxima f_1 =15.00 GHz and f_2 =15.71 GHz at the red and blue arrows correspond to wavenumbers k_1 =89.9 rad μm-1 and k_2 =93.9 rad μm-1 using the calculated spin-wave dispersion (e) at magnetic fields of 26.0 mT (blue curve) and 38.5 mT (red curve). (f) The results of micromagnetic simulations for the y component of the magnetization m_y of Co1 (blue curve) and Co2 (red curve) as a function of t for 29.4 mT and 15.25 GHz. The black arrows indicate zero phase change, i.e. a perfect synchronization. (g) As (f), but for 25.3 mT and 15.30 GHz, leading to $\Delta\phi = \pi/2$.

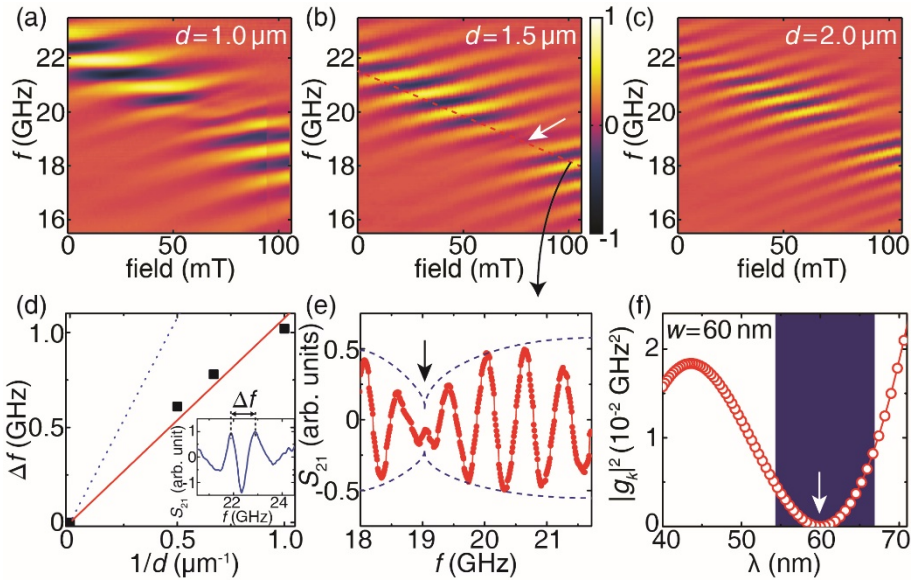

Figure 4 (a)-(c) Transmission spectra S_{21} measured on the sample with $w =$ 60 nm at different propagation distances, namely $d =$ 1.0 μm, 1.5 μm and 2.0 μm. The color scales are identical and shown in (b) only. (d) The frequency intervals Δf extracted at the Co FMR (the inset is from (a)) are plotted as a function of $1/d$. The red solid line and blue dotted line are calculations with and without taking the additional phase jump ϕ_i into account. (e) A cut of the spectrum along the FMR (red dashed line) in (b). The blue dashed envelope is a guide to the eye and the arrow indicates the minimum around 19 GHz. (f) Relative coupling strength calculated as a function of wavelength λ. The blue region shows the range (λ =54.0~66.8 nm) corresponding to (e).